The Journal of Experimental Biology 207, 1093-1099
Published by The Company of Biologists 2004
doi:10.1242/jeb.00852

Intracellular calcium translocation during the contraction–relaxation cycle in scorpionfish swimbladder muscle

Suechika Suzuki[1,*], Naoki Hino[2] and Haruo Sugi[1]

[1]*Department of Physiology, School of Medicine, Teikyo University, 2-11-1, Kaga, Itabashi-ku, Tokyo 173-8605, Japan* and [2]*Department of Physiology, Juntendo Medical College of Nursing, 2-2, Takasu, Urayasu City, Chiba 279-0023, Japan*

*Author for correspondence at present address: Department of Biological Sciences, School of Science, Kanagawa University, 2946 Tsuchiya, Hiratsuka-City, Kanagawa 259-1293, Japan (e-mail: sugi@med.teikyo-u.ac.jp)

Accepted 3 December 2003

Summary

To examine intracellular Ca^{2+} translocation during the contraction–relaxation cycle in vertebrate striated muscle, electron probe X-ray microanalysis was performed on the swimbladder muscle (SBM) fibres of a scorpionfish *Sebastiscus marmoratus*. The SBM fibres were rapidly frozen at rest, during contraction and at various times after the onset of relaxation. Changes in calcium distribution in the components of the sarcoplasmic reticulum (SR) were examined on the SBM fibre cryosections. In resting fibres, the calcium concentration was highest around the boundary between the A and I bands (A–I boundary), where the terminal cisternae (TC) were located. In contracting fibres, the calcium concentration decreased around the A–I boundary, while it increased in all other regions of the sarcomere, indicating Ca^{2+} release from the TC into the myoplasm. During relaxation, the calcium concentration first increased around the regions, where the fenestrated collars (FC) and the longitudinal tubules (LT) were located, and then gradually returned to the levels seen in resting fibres. These results support the view that, after the onset of relaxation in the SBM fibres, Ca^{2+} in the myoplasm is first taken up by the FC and the LT, and then gradually returns to the TC.

Key words: scorpionfish, *Sebastiscus marmoratus*, swimbladder muscle, intracellular Ca translocation, contraction–relaxation cycle, electron probe X-ray microanalysis, sarcoplasmic reticulum, Ca^{2+} release, Ca^{2+} uptake.

Introduction

The contraction–relaxation cycle in all kinds of muscle is controlled by the change in myoplasmic Ca^{2+} concentration (Ebashi and Endo, 1968). In vertebrate skeletal muscle, the myoplasmic Ca^{2+} concentration is regulated by the release of Ca^{2+} from, and its uptake by, the sarcoplasmic reticulum (SR) (Ebashi and Endo, 1968). Using ^{45}Ca autoradiography and quick-freezing techniques, Winegrad (1965, 1968) investigated intracellular Ca translocation during the contraction–relaxation cycle in frog skeletal muscle, and reported that the Ca^{2+} released from the terminal cisternae (TC) of the SR into the myoplasm is taken up at the longitudinal tubules of the SR during relaxation, and then gradually returns to the TC. Subsequent development of electron probe X-ray microanalysis technique has made it possible to study the intracellular Ca distribution with much higher spatial resolution. Somlyo et al. (198l, 1985) performed X-ray microanalysis of cryosections of quick-frozen frog skeletal muscle fibres, and reported, contrary to the result of Winegrad, that Ca^{2+} released from the TC was taken up again by the TC, but not by other SR components. Except within the TC, however, detection of calcium in the other SR components, i.e. the longitudinal tubules (LT) and the fenestrated collars (FC), by X-ray microanalysis is extremely difficult because of poor preservation of these structures in cryosections. Therefore, the above discrepancy concerning the $[Ca]_i$ translocation still remains to be settled.

In striated muscles of teleosts, both the SR and the myofibrils are extremely well aligned in the transverse direction, so that the well-developed SR components are invariably located at the same regions in each sarcomere (Fawcett and Revel, 1961). The present work was undertaken to give clear information about intracellular Ca translocation during the contraction–relaxation cycle in vertebrate striated muscle, using the swimbladder muscle (SBM) of a scorpionfish *Sebastiscus marmoratics*. The extremely well aligned SR components in the SBM fibres provide an opportunity to determine the calcium distribution in the SR components during the contraction–relaxation cycle by quantitative X-ray microanalysis of SBM fibre cryosections. It is shown that, in SBM fibres, calcium released from the TC

is taken up by the LT and the FC of the SR, thus supporting the observations of Winegrad (1965, 1968) in frog skeletal muscle.

Materials and methods

Fibre preparation

Adult scorpionfish *Sebastiscus marmoratus* Cuvier et Velenciennes (body length 16–20 cm) were collected at Sagami Bay, Japan, and kept in seawater at 17°C. Animals were killed by decapitation and the swimbladder in the abdomen exposed. A pair of swimbladder muscles run along both sides of the swimbladder. A small bundle consisting of 3–5 SBM fibres (~20 mm length, ~0.3 mm diameter) with tendons attached to both ends, was dissected from the posterior part of the SBM. The experimental solution (fish Ringer) had the following composition (in mmol l^{-1}): NaCl, 167.5; KCl, 4.4; $CaCl_2$, 2.2; $MgCl_2$, 1.3 (pH adjusted to 7.2 using 10 mmol l^{-1} Hepes-Tris buffer).

Quick-freezing

The method used for quick-freezing the SBM fibres was essentially the same as in our previous study (Suzuki et al., 1993). Briefly, the preparation was mounted horizontally in an experimental chamber filled with the experimental solution (17–20°C); one end of the preparation was clamped, while the other end was connected to a strain gauge (UL-2, Shinko, Tokyo, Japan) to record isometric force. The middle portion of the fibres was placed in a narrow space between two gold plates (Balzer, Liechtenstein), closely facing each other. The fibres were made taut by stretching them to ~1.2 times the slack length (sarcomere length, ~2.5 μm).

SBM fibres were quick-frozen at rest, during isometric tetanus, and at 0.1, 1, 3 and 5 s after onset of relaxation. The fibres were made to contract isometrically by applying supramaximal AC current (100 Hz) through the connections at both fibre ends, and recording the isometric forces on a chart recorder (Graphtec, Tokyo, Japan). Before freezing, the experimental solution in the chamber was drained, and the fibres were quick-frozen by jetting liquid propane (~190°C) from two nozzles to the gold plates and the fibres. The frozen fibres were removed from the experimental chamber together with the two gold plates, and put into liquid N_2 to be stored until cryosections were cut.

Cryosections

Longitudinal cryosections (~200 nm thick) were cut from the frozen SBM fibres at –110°C on a cryoultramicrotome (LKB Nova; LKB Produkter, Bromma, Sweden), and then carefully sandwiched between two cooled Ni-grids with thin carbon films. In the cryochamber kept at –125°C, the Ni-grid sandwich was transferred to a freeze-drying aluminium container, equipped with a thermoelectric device to monitor temperature during freeze drying. The mass of the container was enough to maintain temperatures below –95°C for 24 h in a vacuum chamber. The freeze-drying container was then brought out of the cryochamber, further cooled to –196°C with liquid N_2, and then put into the vacuum chamber of a freeze-drying machine (FD-2A; Eiko Engineering, Tokyo, Japan) to be freeze-dried at 10^{-6} torr (1.3×10^{-4} Pa) and at –95°C for 24 h. After the freeze-drying procedure, the Ni-grid sandwich was split apart, and the cryosections were lightly evaporated *in vacuo* with carbon for X-ray microanalysis.

Electron probe X-ray microanalysis

Electron probe X-ray microanalysis was performed using an analytical electron microscope (JEM 2000FXS, JEOL, Tokyo, Japan) equipped with an energy dispersive X-ray microanalyzer (TN5450; Tracor Northern Inc., Middleton, Wisconsin, USA). Initially, the cold trap attached to the electron microscope column was cooled with liquid N_2 to avoid specimen contamination. The freeze-dried cryosections on the Ni-grid were mounted on a Be-stage of the cryotransfer holder (EH-CTH 10; JEOL), and put into the electron microscope, the cryosections being cooled at –130°C by a supply of liquid N_2. The transmission system of the analytical electron microscope was operated at an accelerating voltage of 80 kV. For X-ray microanalysis (spot analysis), the electron beam was focused on a fixed area (diameter, 0.16 μm) under a magnification of 25 000× with a sample current of ~1.35 nA. X-ray emissions from the cryosection were collected for a period of 200 s. To examine whether or not mass-loss and/or contamination in the cryosection occurred during the collection of X-ray emissions, the change of spectral peak integral during the course of analysis was monitored using a software program (Mass-loss monitoring mode) of the TN5450 computer system, which detected any significant mass-loss and contamination that occurred during the analysis.

The elemental concentrations were calculated from X-ray spectra in mmol kg^{-1} dry mass, based on the Hall's quantitative equation (Hall, 1971; Shuman et al., 1976). X-ray emissions of up to ~10.24 KeV were collected, and the intensity of X-ray continuum was represented by an integral X-ray count in a region of 4.5–5.5 KeV where no spectral peak appeared. For each X-ray spectrum, a reference spectrum was obtained from the area including only carbon supporting film. To calculate elemental concentrations, the intensity of X-ray continuum from the cryosection was always corrected by subtracting the artificial X-ray continuum caused by carbon film, Ni-grid and other factors (e.g. contamination of Si) from the X-ray spectrum.

To determine the intensity of each spectral peak with reasonable accuracy, elemental spectral peaks were subjected to a multiple least-squares fit to corresponding elemental standard spectral peaks (Na, Mg, Al, Si, P, S, Cl, K, Ca and Ni), obtained by analyzing pure chemicals, and stored in the TN5450 computer system. In the case of overlapped spectral peaks such as K-K_β and Ca-K_α emissions, the first and the second derivatives of the spectral peaks were further subjected to a multiple least-squares fit to the derivatives of the standard spectral peaks.

Conventional electron microscopy

SBM fibres in resting muscle were fixed with a 2.5% glutaraldehyde solution containing 2 mmol l^{-1} $CaCl_2$ (adjusted to pH 7.2 with 0.1 mol l^{-1} cacodylate buffer), and postfixed with a 2% osmium tetroxide (OsO_4) solution in the same buffer (Suzuki et al., 2003). The preparations were then dehydrated through a graded ethanol series, cleared with propylene oxide, and embedded in Epon 812. Ultrathin sections cut on a Porter Blum MT-2 ultramicrotome (DuPont Instrument-Sorval, Wilmington, Delaware, USA) were stained with uranyl acetate and lead citrate, and examined using a JEOL JEM 2000FXS transmission electron microscope.

Results

Arrangement of the SR components in the sarcomere of the SBM fibres

Fig. 1A shows a typical conventional electron micrograph of the longitudinal section at the middle region of the SBM fibre. The SBM fibres are thick (diameter, ~150 μm), and both the myofibrils and the SR are extremely well aligned in the transverse direction. The T-tubules are located at the boundary between the A and I bands (A–I boundary), so that there are two T-tubules in each sarcomere, except for the fibre ends where the T-tubules are located at the Z-line level (Suzuki et al., 2003). Fig. 1B illustrates the arrangement of the SR components in a half sarcomere. At the A–I boundary, two TCs

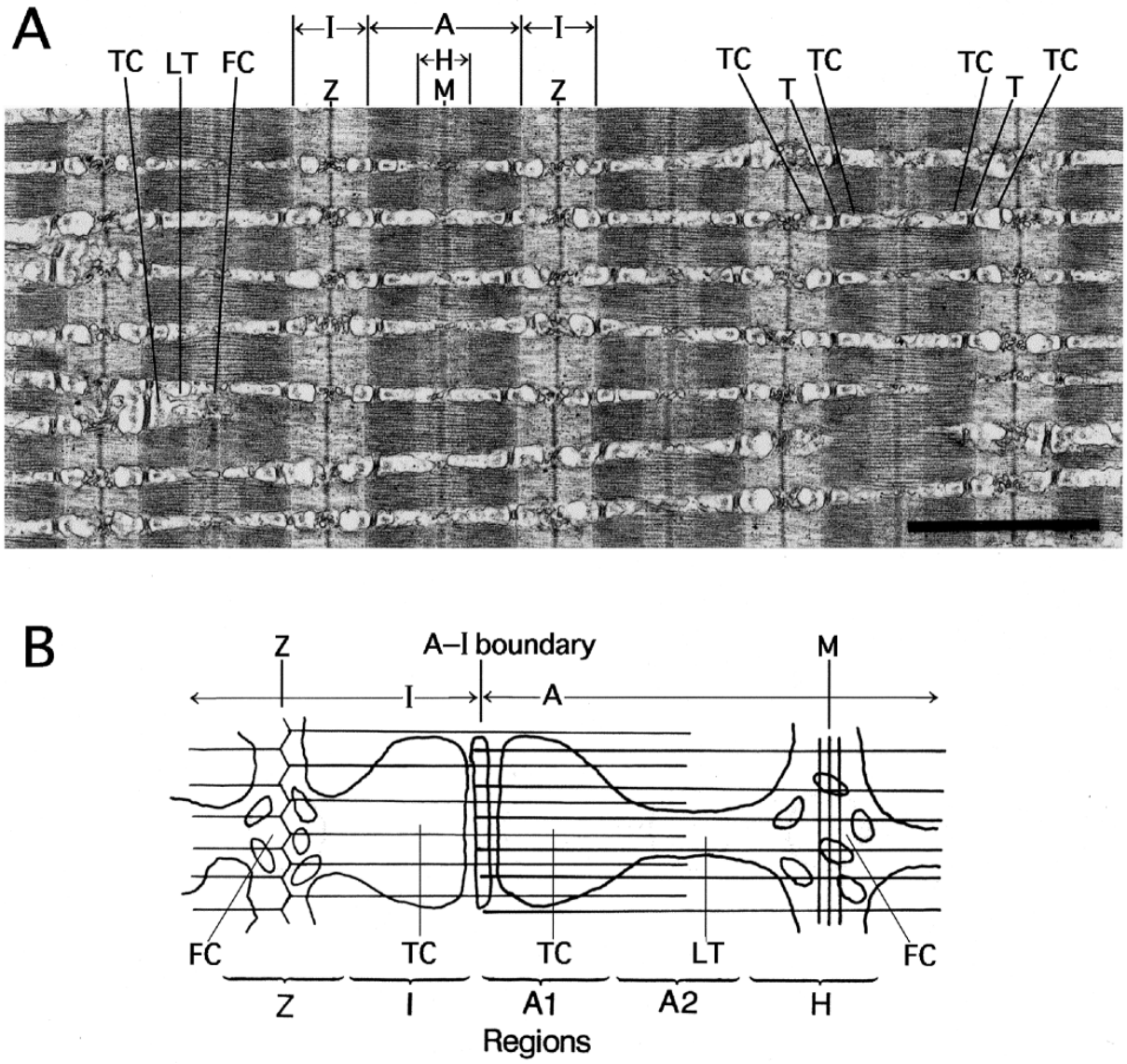

Fig. 1. Arrangement of the SR components along the half sarcomere in SBM fibres. (A) Conventional electron micrograph of the fibre longitudinal section, showing the regular striation pattern (I, I band; Z, Z line; A, A band; H, H zone; M, M line) and regular arrangement of the SR components. LT, longitudinal tubules; FC, fenestrated collars; TC, terminal cisternae; T, transverse tubule. Bar, 2 μm. (B) Diagram illustrating the arrangement of the SR components and the five consecutive regions along the half sarcomere.

are in close apposition to a T-tubule to form the triad. The FC is located around the Z-line level and H-zone. The LT of the SR extends from the A–I boundary to the H-zone.

Intracellular Ca distribution in resting SBM fibres

A typical example of longitudinal cryosections of the SBM fibres is shown in Fig. 2. Although striation patterns are clearly visible, it was not possible to observe the SR components in SBM fibre cryosections. We therefore performed spot analysis to measure Ca concentrations in the SR components, assuming that the cryosections contain the SR components as well as the myofibrils.

This assumption was proved valid for the following reasons: (1) in resting fibres, the Ca concentration was always highest around the A–I boundary, where the TC of the SR were located (see Fig. 4 and Table 2), (2) spot analysis on 20 consecutive regions along the A–I boundary in the transverse direction revealed that regions of high [Ca] (>20 mmol kg^{-1} dry mass) were not continuous but separated from each other by regions of low [Ca] (Fig. 3), reflecting the separation of the SR by the myofibrils (Fig. 1A).

Thus, the distribution of Ca in the SR components of resting fibres was determined by spot analysis at the centre of five consecutive regions along the half sarcomeres, i.e. the Z region, containing the FC; I and A1 regions, containing the TC; A2 region, containing the LT; and H region, containing the FC (Figs 1B, 2). As can be seen in Fig. 4A, the [Ca] in the I and A1 regions (42.7±5.0 and 43.6±5.4 mmol kg^{-1} dry mass, means ± S.E.M., N=36, respectively), were much higher than those in the Z, A2 and H regions (23.7±2.1, 13.3±2.1 and 9.9±1.7 mmol kg^{-1} dry mass, respectively, N=36) (P<0.001).

Table 1 shows concentrations of several elements including Ca in the five consecutive regions of resting fibres. Except for Ca, the concentrations of all the elements were nearly constant in all the five regions. The high K and low Na concentrations indicate that the fibres had been frozen without any serious damage to the surface membrane. The concentrations of elements other than Ca did not change significantly whether the fibres were frozen during contraction or at various times after the onset of relaxation.

Intracellular Ca distribution in contracting SBM fibres

The SBM fibres were quick-frozen at various stages of the contraction–relaxation cycle, and the Ca concentrations in the five regions along the half sarcomere at these various stages are summarized in Table 2. In fibres frozen at the peak of the

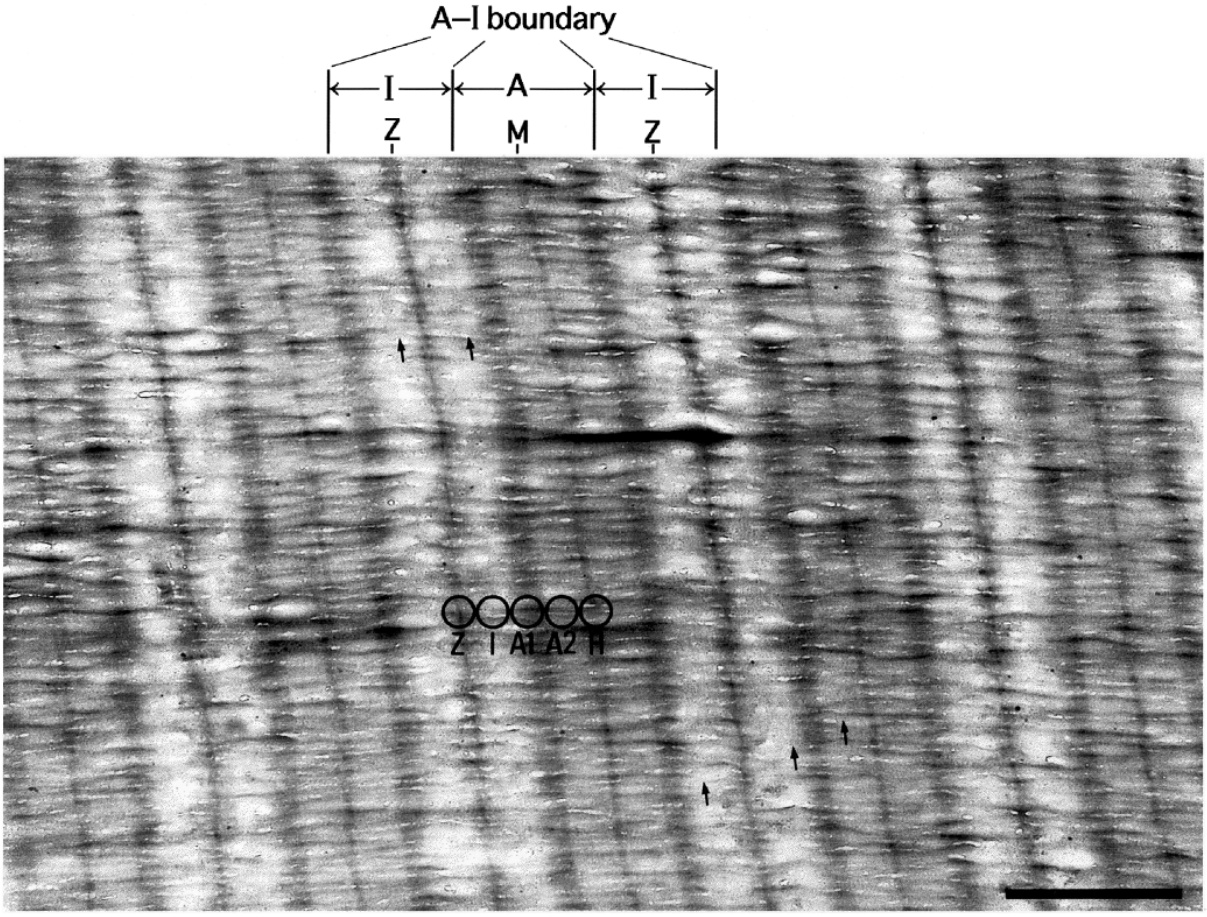

Fig. 2. Typical longitudinal cryosection of an SBM fibre, exhibiting the regular striation pattern. Five consecutive regions along the half sarcomere (Z, I, A1, A2 and H) are indicated at the centre. The SR and T tubules are barely visible (arrows). Bar, 2 μm.

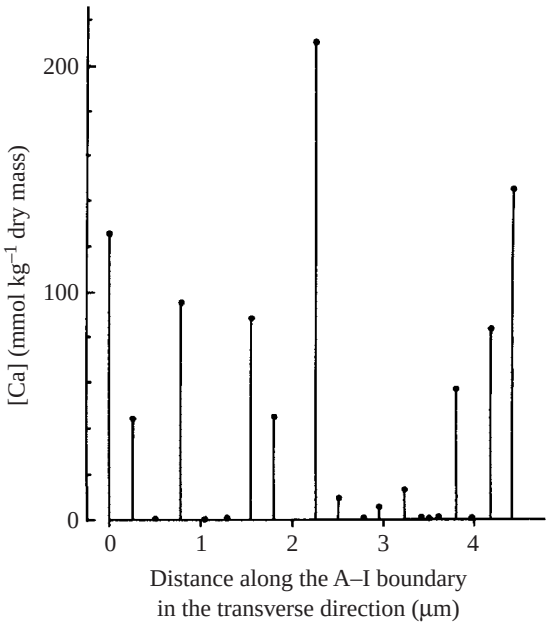

Fig. 3. Distribution of Ca along the A–I boundary in the transverse direction. Note that the regions of high [Ca] are separated by those of low [Ca].

mechanical response to electrical stimulation, the [Ca] in the A1 region (19.8±2.7 mmol kg^{-1} dry mass, N=25) was significantly lower than that in resting fibres (P<0.01), while the [Ca] in the H region (16.5±2.3 mmol kg^{-1} dry mass, N=25) was significantly higher than that in resting fibres (P<0.05) (Fig. 4B, Table 2). [Ca] in the Z, I and A2 regions did not change significantly from the corresponding values in resting fibres, though the mean [Ca] in the I region decreased to 31.5 mmol kg^{-1} dry mass, and that in the A2 region increased to 16.1 mmol kg^{-1} dry mass.

These results are consistent with the release of Ca from the TC into the myoplasm, if the increase in [Ca] in the Z, A2 and H regions is interpreted as being due to the increase in the myoplasmic [Ca^{2+}] in these regions. The insignificant changes in [Ca] in the Z and I regions may be a consequence of the distance between the TC and FC being too short in these regions.

Intracellular Ca distribution after onset of relaxation

SBM fibres were frozen at various times after onset of relaxation. At 0.1 s after onset of relaxation, the isometric force fell to ~50% of the maximum value. In fibres quick-frozen at this stage, [Ca] in the A1, A2 and H regions were significantly higher than the corresponding values in contracting fibres (P<0.05 for the A1 and A2 regions and P<0.01 for the H region; Table 2).

The isometric force fell to zero at 1 s after onset of relaxation. In fibres quick-frozen at this stage, the [Ca] in the H region was significantly lower than the value in the previous stage (P<0.05), while the [Ca] in the other regions did not change significantly (Fig. 4D; see also Table 2). In fibres frozen at 3 and 5 s after onset of relaxation (or at ~2 s and ~4 s after completion of relaxation), [Ca] in the five regions gradually returned to the values in resting fibres (Fig. 4E,F and Table 2); thus, [Ca] in all the five regions at 5 s after onset of relaxation did not differ significantly from the corresponding values in resting fibres.

Discussion

Ca localization in the TC of resting SBM fibres

Based on the arrangement of the SR components along each half sarcomere in the SBM fibres (Fig. 1A,B; Suzuki et al., 2003), we have succeeded in measuring the [Ca] in each SR component on the longitudinal cryosections of quick-frozen SBM fibres by spot analysis of the five consecutive regions corresponding to the SR components along the half sarcomere (Fig. 2). In resting fibres, the [Ca] in the I and A1 regions were much higher than in the other regions (Fig. 4A, Tables 1, 2), reflecting the localization of Ca at high concentrations in the lumen of the TC on both sides of the T-tubule.

The [Ca] in the TC obtained in the present study (~40 mmol kg^{-1} dry mass) is much smaller than the value reported for the TC in resting frog muscle fibres (117 mmol kg^{-1} dry mass; Somlyo et al., 1981). In frog skeletal muscle fibres, however, the SR volume is less than 5% of the whole fibre volume (Peachey, 1965; Mobley and Eisenberg, 1975), whereas the SR volume in SBM fibres is ~25% of the whole fibre volume (Suzuki et at., 2003). Taking this into consideration, the total amount of Ca in the TC lumen

Table 1. *Concentrations of various elements at the five regions along the half sarcomere in resting fibres*

	Region				
Element	Z	I	A1	A2	H
Ca	23.7±2.1	42.7±5.0	43.6±5.4	13.3±2.1	9.9±1.7
K	654.1±49.3	679.3±45.9	694.7±41.2	641.6±36.2	671.2±49.5
Cl	141.6±22.2	153.3±17.5	151.7±15.0	151.9±14.1	164.7±26.1
P	386.1±25.0	417.4±24.7	398.1±24.6	333.8±18.9	357.6±25.5
Mg	67.2±4.6	66.7±5.1	76.2±5.5	74.3±4.8	77.2±6.5
Na	77.5±16.8	82.0±13.0	77.2±12.8	68.6±9.4	86.1±16.7

Values are mmol kg^{-1} dry mass (mean±S.E.M., N=36).
See text for a description of the regions.

Table 2. *Ca concentrations at the five regions along the half sarcomere at various stages of the contraction–relaxation cycle*

State	Region Z	I	A1	A2	H	*N*
Resting	23.7±2.1	42.7±5.0	43.6±5.4	13.3±2.1	9.9±1.7	36
Contracting	22.5±3.3	31.5±4.4	19.8±2.7**	16.1±2.4	16.5±2.3*	25
Time after onset of relaxation (s)						
0.1	34.8±4.0*	39.8±5.6	29.8±4.1*	28.8±5.2*	35.8±5.6**	26
1.0	26.9±4.6	38.6±3.4	31.5±5.4	21.2±3.8	20.4±3.0*	23
3.0	18.1±2.7	47.8±4.3	34.4±3.1	10.2±1.8*	5.8±1.3**	31
5.0	22.6±4.3	56.9±5.6	59.6±5.8**	8.1±2.9	7.4±2.2	20

Values are mmol kg^{-1} dry mass (mean±S.E.M.). Significance of the differences from the value in the previous stage are also shown; *P<0.05, **P<0.01.

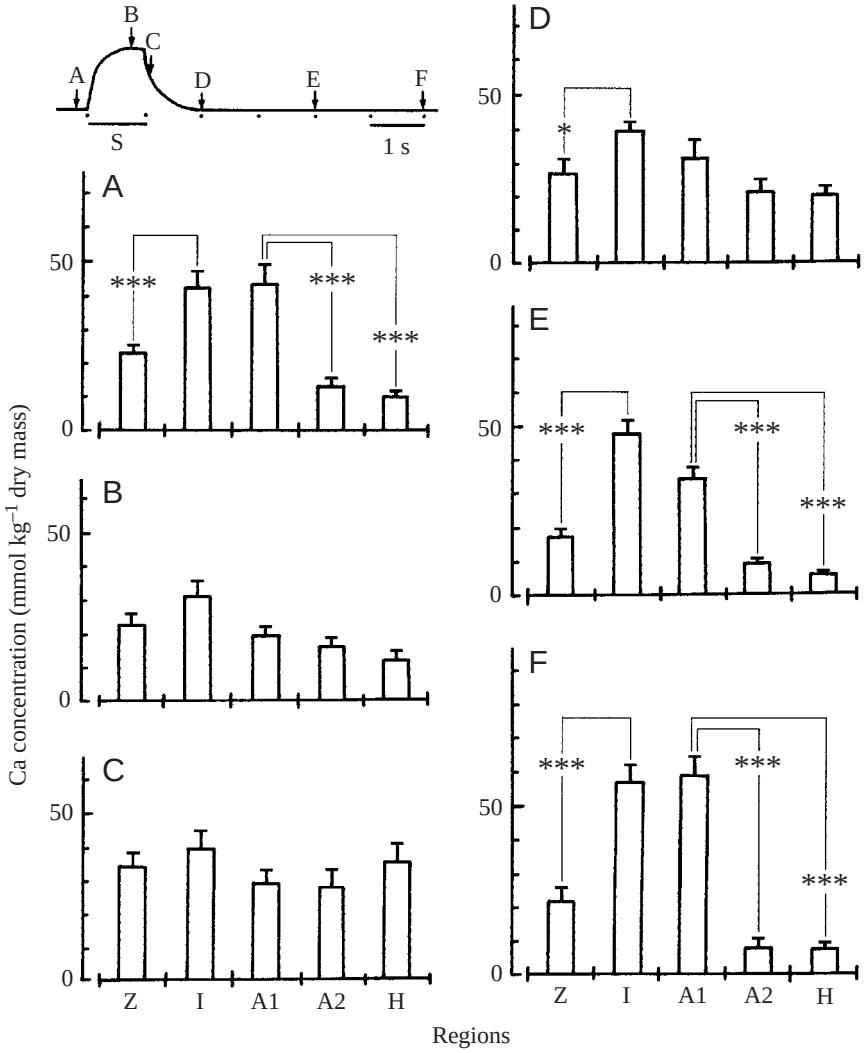

Fig. 4. Ca distribution in the five regions at various stages in the contraction–relaxation cycle. Inset (top) is a diagram illustrating the six different stages of force change used for quick-freezing, i.e. at rest (A), during contraction (B), and at 0.1 s (C), 1 s (D), 3 s (E) and 5 s (F) after onset of relaxation. The bar shows period of stimulation (S). (A–F) [Ca] in the five regions along the half sarcomere. Values are means ± S.E.M. (N=36). Significant differences in [Ca] in the five regions are also shown; *P<0.05; ***P<0.001.

in the SBM fibres may be rather larger than that in frog fibres.

Release of Ca from the TC into the myoplasm

In SBM fibres quick-frozen at the peak of mechanical response to electrical stimulation, the [Ca] in the A1 region was significantly smaller than the corresponding value in resting fibres (P<0.01), while the [Ca] in the H region was significantly higher (P<0.05) (Fig. 4B, Table 2). The mean [Ca] in the A2 region was also higher than that in resting fibres, though the difference was not significant. These results can be taken to reflect Ca release from the TC into the myoplasm, if the increased [Ca] is assumed to result from increased myoplasmic [Ca^{2+}] around the SR.

We calculated an approximate estimate of the amount of Ca released from the TC to the myoplasm from the difference in mean [Ca] of the I and A1 regions in resting and contracting fibres (43.2–26.7=17.5 mmol kg^{-1} dry mass). Assuming that the TC volume is ~60% of the SR volume (Suzuki et al., 2003), the dilution rate of released Ca is ~0.15. Consequently, the myoplasmic concentration of the released Ca is ~2.6 mmol kg^{-1} dry mass (17.5×0.15). If the water content of the SBM fibres is assumed to be ~70% (Somlyo et al., 1981), the 2.6 mmol kg^{-1} dry mass is equivalent to 1.11 mmol l^{-1} fibre H_2O, a value nearly equal to that reported for frog muscle fibres (~1 mmol l^{-1} fibre H_2O; Somlyo et al., 1981).

Uptake of Ca by the SR components

In the fibres frozen at 0.1 s after onset of

relaxation, the [Ca] in the Z, A1, A2 and H regions were significantly higher than the corresponding values in resting fibres ($P<0.05$ for the Z, A1 and A2 regions and $P<0.01$ for the H region) (Fig. 4C, Table 2). These results are consistent with all the SR components starting to take up the myoplasmic Ca^{2+} at the early phase of relaxation. At 1 s after onset of relaxation, the [Ca] in the H region became significantly smaller than the value at the previous stage of relaxation ($P<0.05$) (Fig. 4D, Table 2). The mean [Ca] was also smaller in the Z and A2 regions, and larger in the I and A1 regions (Fig. 4D, Table 2). At 3 s after onset of relaxation, the [Ca] in the A2 and the H regions decreased significantly compared to the values at the previous stage ($P<0.05$ and 0.01, respectively) (Fig. 4E, Table 2). The mean [Ca] was also decreased in the Z region, but increased in the I and A1 regions (Fig. 4E, Table 2). These results seem to indicate that the Ca, already taken up by the LT and FC in the previous stage, is moving to the TC.

At 5 s after onset of relaxation, the [Ca] in the A1 region became significantly higher than the value at the previous stage ($P<0.05$), and the mean [Ca] in the I region was also higher than the value at the previous stage. Thus, the [Ca] in both the I and A1 regions returned to levels much higher than those in all the other regions ($P<0.001$) (Fig. 4F, Table 2), indicating that the Ca distribution along the SR components returned to that seen in resting fibres within 5 s after the onset of relaxation.

Mechanism of the Ca translocation in the SR components during relaxation

In the present study, we have clearly answered the question of whether the myoplasmic Ca^{2+} is taken up by the LT (Winegrad, 1965, 1968) or by the TC (Somlyo et al., 1981) during relaxation of vertebrate striated muscle fibres. The answer we have obtained is intermediate between the above two cases; after onset of relaxation in the SBM fibres, the myoplasmic Ca^{2+} is taken up not only by the LC and FC but also by the TC (Fig. 4, Table 2), which is consistent with the uniform distribution of Ca pump proteins all over the SR membrane except for the triadic junctional region (Jorgensen et al., 1979; Saito et al., 1984). As can be seen in Fig. 4C–F and Table 2, the increases in [Ca] in the Z, A1, A2 and H regions, reflecting Ca uptake by all the SR components, are most prominent in the early phase of relaxation (at 0.1 s after its onset). The reason why Somlyo et al. (1981) did not observe Ca uptake by the LC and FC might be partly because they did not measure [Ca] during relaxation, and partly because the LT and FC are much less developed in frog muscle fibres than in SBM fibres.

Muscle fibres of cold-blooded animals are known to contain parvalbumin, a Ca-binding protein buffering the myoplasmic [Ca^{2+}] (Gillis, 1985). If parvalbumin is present in SBM fibres, it may increase the rate of relaxation to a certain extent. However, possible Ca^{2+}-binding to parvalbumin may not qualitatively affect the present results, since parvalbumin distributes uniformly in the myoplasm.

In vertebrate skeletal muscle, the Ca in the TC lumen is largely bound to the Ca-binding protein calsequestrin, localized at high concentrations in the TC (Meissner, 1975; Jorgensen et al., 1979; Guo and Campbell, 1995). In toadfish SBM, however, a small concentration of calsequestrin is also present in the LC (Franzini-Armstrong et al., 1987). These reports suggest that calsequestrin concentration is highest in the TC and lowest in the FC. It therefore seems likely that the Ca taken up by all the SR components during relaxation gradually moves towards the TC along the calsequestrin concentration gradient. Much more experimental work is needed to prove the mechanism of intracellular translocation stated above.

The authors thank Mr Shohei Kouno, TEC-Center for Analytical Systems, Sumi-Sho Electronics Co., Toda-City, Japan, for his technical assistance with an inductively coupled plasma spectrometer.

References

Ebashi, S. and Endo, M. (1968). Calcium ion and muscle contraction. *Prog. Biophys. Mol. Biol.* **18**, 123-183.

Fawcett, D. W. and Revel, J. P. (1961). The sarcoplasmic reticulum of a fast-acting fish muscle. *J. Cell Biol.* **10 Suppl**, 89-109.

Franzini-Armstrong, C., Kenny, L. J. and Varriana-Marston, E. (1987). The structure of calsequestrin in triads of vertebrate skeletal muscle: A deep-etch study. *J. Cell Biol.* **105**, 49-56.

Gillis, J. M. (1985). Relaxation of vertebrate skeletal muscle. A synthesis of the biochemical and physiological approaches. *Biochem. Biophys. Acta* **811**, 97-145.

Guo, W. and Campbell, K. P. (1995). Association of triadin with the ryanodine receptor and calsequestrin in the lumen of the sarcoplasmic reticulum. *J. Biol. Chem.* **270**, 9027-9030.

Hall, T. A. (1971). The microprobe assay of chemical elements. In *Physical Techniques in Biological Research* (ed. G. Oster), pp. 157-275. New York: Academic Press.

Jorgensen, A. O., Kalnins, V. and MacLenan, D. H. (1979). Localization of sarcoplasmic reticulum proteins in rat skeletal muscle by immuno-fluorescence. *J. Cell Biol.* **80**, 372-384.

Meissner, G. (1975). Isolation and characterization of two types of sarcoplasmic reticulum vesicles. *Biochim. Biophys. Acta* **389**, 51-68.

Mobley, B. A. and Eisenberg, B. R. (1975). Sizes of components in frog skeletal muscle measured by methods of stereology. *J. Gen. Physiol.* **66**, 31-45.

Peachey, L. D. (1965). The sarcoplasmic reticulum and transverse tubules of the frog's sartorius. *J. Cell Biol.* **25**, 209-231.

Saito, A., Seiler, S., Chu, A. and Fleischer, S. (1984). Preparation and morphology of sarcoplasmic reticulum terminal cisternae from rabbit skeletal muscle. *J. Cell Biol.* **99**, 875-885.

Shuman, H., Somlyo, A. V. and Somlyo, A. P. (1976). Quantitative electron probe microanalysis of biological thin sections: methods and validity. *Ultramicroscopy* **1**, 317-339.

Somlyo, A. V., Gonzalez-Serratos, H., Shuman, H., McClellan, G. and Somlyo, A. P. (1981). Calcium release and ionic changes in the sarcoplasmic reticulum of tetanized muscle: an electron-probe study. *J. Cell Biol.* **90**, 577-594.

Somlyo, A. V., McClellan, G., Gonzalez-Serratos, H. and Somlyo, A. P. (1985). Electron probe X-ray microanalysis of post-tetanic Ca^{2+} and Mg^{2+} movements across the sarcoplasmic reticulum *in situ*. *J. Biol. Chem.* **260**, 6801-6807.

Suzuki, S., Oshimi, Y. and Sugi, H. (1993). Freeze-fracture studies on the cross-bridge angle distribution at various physiological states and the thin filament stiffness in single skinned frog muscle fibers. *J. Electron Microsc.* **42**, 107-116.

Suzuki, S., Hino, N. and Sugi, H. (2003). Ultrastructural organization of the transverse tubule and the sarcoplasmic reticulum in a fish sound-producing muscle. *J. Electron Microsc.* **52**, 337-347.

Winegrad, S. (1965). Autoradiographic studies of intracellular calcium in frog skeletal muscle. *J. Gen. Physiol.* **48**, 455-479.

Winegrad, S. (1968). Intracellular calcium movements of frog skeletal muscle during recovery from tetanus. *J. Gen. Physiol.* **51**, 65-83.